

## ARTICLES

**Comparison of the high-pressure and low-temperature structures of ethanol and acetic acid**

David R. Allan

*Department of Physics and Astronomy, The University of Edinburgh, Mayfield Road, Edinburgh EH9 3JZ, United Kingdom*

Stewart J. Clark

*Department of Physics, The University of Durham, Science Laboratories, South Road, Durham DH1 3LE, United Kingdom*

(Received 6 January 1999; revised manuscript received 27 April 1999)

We have determined the high-pressure crystal structures of ethanol and acetic acid, including the positions of the hydrogen atoms, using a combination of single-crystal x-ray-diffraction techniques and *ab initio* pseudo-potential calculations. We find that in the high-pressure structure of ethanol the molecules are arranged in infinite hydrogen-bonded chains that adopt a structural conformation that is distinctly different from that of the low-temperature form. The hydrogen-bond lengths and bond angles within the chains are equal by symmetry and, as the molecules also have an alternating alignment to the chains, the molecular chains are relatively unstrained. It is proposed that this uniformity and lack of strain within the chains enables ethanol to crystallize much more readily than methanol at high pressure. For acetic acid we find that the molecules are also arranged in infinite hydrogen-bonded chains that are essentially identical to those in the low-temperature structure. However, they adopt markedly different relative orientations, which leads to a more efficient molecular packing and a radically different methyl-methyl contact motif between adjacent molecular chains. The calculated enthalpies of the high-pressure and low-temperature structures show that the high-pressure phase is the most energetically favorable. We find a relatively small 0.056 eV/molecule enthalpy difference between the two structures and this is reflected in the very low freezing pressure of approximately 0.2 GPa at room temperature compared to the freezing temperature of 16 °C at ambient pressure. [S0163-1829(99)03233-6]

**I. INTRODUCTION**

The range of intermolecular interactions, in conjunction with molecular form and symmetry, are strongly coupled to the structure and dynamics of molecular solids. As these interactions strongly depend on intermolecular distances, high pressure provides a powerful probe for the study of molecular solids<sup>1</sup> as these distances, and hence the interactions, can be altered substantially. In order to develop a systematic understanding of hydrogen-bonded molecular systems at high pressure, it is vital that a range of hydrogen-bonded small-molecule systems are studied. We have recently presented the high-pressure structures of methanol and formic acid<sup>2,3</sup> where we demonstrated that the structures are not only substantially different from those formed at low temperature but also in methanol the potential for vitrification at high pressure is related to the increased strain the molecular chains and for formic acid the molecular orientations in the high-pressure crystal structure offers a clear route to dimer formation at more elevated pressures.

Here we present the high-pressure structures of ethanol and acetic acid. The low-temperature structures of both of these systems are composed of linear hydrogen-bonded chains of molecules and they are the last in their respective series to do so; in the linear monoalcohols the larger molecules all form glasses on cooling, and in the linear monocarboxylic acids all the molecules larger than acetic acid form crystal structures composed of isolated dimers.

The linear alcohols  $\text{H}(\text{CH}_2)_n\text{OH}$  interact through a combination of a short-range repulsive force, a steric interaction, a weak van der Waals attraction, and relatively strong directional hydrogen bonds. As the relative influence of hydrogen bonding is expected to decrease with increasing molecular length, competition between these forces is expected to vary with  $n$ . This competition can result in a variety of interesting structural effects and for other monoalcohol systems ( $\text{C}_n\text{H}_m\text{OH}$ ) chain, ring, and dimer conformations can result.<sup>4</sup>

For methanol, which is the simplest linear alcohol with  $n=1$  ( $\text{H}(\text{CH}_2)_1\text{OH}$ ), two orthorhombic crystalline phases are formed on cooling—the  $\beta$  phase crystallizes below 175 K and transforms to the  $\alpha$  phase at about 157 K on further cooling.<sup>5,6</sup> For ethanol [ $\text{H}(\text{CH}_2)_2\text{OH}$ ], only a single-crystalline phase, with the monoclinic space group  $Pc$ , is observed on cooling below the freezing temperature of  $\sim 156$  K (Ref. 7) at atmospheric pressure. The low-temperature structures of both methanol and ethanol are characterized by infinite hydrogen-bonded molecular chains with the molecules arranged in an alternating sequence.

At ambient temperature, the equilibrium freezing pressure of methanol is 3.5 GPa, although, in practice, it is very easy to superpress the liquid phase. The nucleation rate for crystal growth rises to a maximum near 7 GPa before vanishing at 10.5 GPa.<sup>8,9</sup> If the liquid is rapidly compressed beyond 10.5 GPa, crystallization does not occur and the liquid becomes a pressure-induced glass.<sup>8,9</sup> However, at ambient pressure methanol cannot be vitrified by rapid cooling of the bulk

liquid, but only by vapor deposition on a cold substrate (see, e.g., Ref. 10). The high-pressure crystal structure of methanol has recently been solved and has been used to determine which structural aspects may explain why methanol is difficult to crystallize at high pressure and so readily forms a glass.<sup>2</sup> The most striking feature of the high-pressure structure was found to be the conformation of the hydrogen-bonded chains of molecules. The molecules are sequenced so that two neighboring molecules are aligned parallel to one another, forming a hydrogen-bonded pair, while a third is aligned antiparallel and correspondingly shifted by its own length to form a hydrogen bond between each pair. This “2-1-2-1” sequence is unique to the observed chain conformations in monoalcohol systems and leads to considerable strain within the high-pressure methanol structure.<sup>2</sup>

Ethanol, in contrast, crystallizes readily at high pressure, with Raman-scattering studies indicating that the high-pressure phase is stable from about 1.9 GPa to at least 17 GPa.<sup>11,12</sup> Shimizu *et al.*<sup>12</sup> observed remarkable negative shifts in the OH stretching frequencies with pressure, which they interpreted as being due to the increasing strength of the hydrogen bonds in the chains (or the *increase* in the O-H bond length). The negative values of  $dv/dP$  for the O-H stretch frequencies  $\nu$  were found to be smaller than those of other molecular solids with one-dimensional chains. It was suggested that nonbonding interactions involving the large  $\text{CH}_3\text{CH}_2$  group in ethanol impede the compression of the chain — although this notion was based on ethanol retaining the low-temperature structure at high pressure.

The monocarboxylic acids formic acid ( $\text{HCOOH}$ ) and acetic acid ( $\text{CH}_3\text{COOH}$ ) distinguish themselves from the other, larger molecules in the series in that they form crystal structures at low temperatures with infinite hydrogen-bonded molecular chains rather than isolated dimer pairs linked by relatively weak intermolecular bonding. Both formic acid and acetic acid crystallize in the  $Pna2_1$  space group at temperatures of 8 °C and 16 °C, respectively, with remarkably similar conformations of the carboxyl groups within the chains—the structures being essentially identical with the exception of the methyl group in acetic acid.

In a recent study of the high-pressure phase<sup>3</sup> of formic acid, it was found that the molecules also form infinite hydrogen-bonded chains although they adopt both the *cis* and *trans* conformers rather than only the *trans* form of the low-temperature phase. The molecules are arranged in pairs on symmetrically flat layers so that “near dimers” are created between adjacent molecules in the same chain—though the required bond lengths for “true dimer” formation are significantly shorter than those observed. We anticipate that the transition observed at 4.5 GPa, in the high-pressure Raman study of Shimizu<sup>13</sup> on the deuterated form ( $\text{DCOOD}$ ), is due to the creation of either bonds between these neighboring molecules so that dimers are created or between adjacent chains so that a hydrogen-bonded network is formed.

Here we report the first high-pressure structure determinations of ethanol and acetic acid where we use a combination of single-crystal diffraction and *ab initio* density-functional calculations. Both methods are required to fully determine the structures since the x-ray diffraction methods determine the space group, unit cell, and C and O positions that are unlikely to be found from *ab initio* methods and the

DFT calculations are required to obtain accurate atomic coordinates of the hydrogens.

We find that the ethanol structure is monoclinic with  $P2_1/c$  symmetry and the hydrogen-bonded chains adopt a relatively unstrained 1-1-1 arrangement. We propose that the relative uniformity and lack of strain within the chains allows ethanol to crystallize much more readily than methanol at high pressure. Although the distribution of bond angles (i.e., the strain in the hydrogen bonds) increases for methanol at high pressure the contrary is found for ethanol where the hydrogen-bonded chains are more regular than those of the low-temperature phase. Unlike the behavior of methanol, this observation is the reverse of what is expected from the computer simulation results of Root and Berne<sup>14</sup> that predict that the range of hydrogen-bond angles increases with pressure.

For acetic acid, we find that, despite the low-freezing pressure of only 0.2 GPa, the high-pressure crystal structure is quite different from that formed at low temperature. Although the hydrogen-bonded molecular chains of the high-pressure structure are virtually identical to those of the low-temperature phase, the relative orientations of the chains are markedly different. The chains reorient in such a manner that puckered molecular layers are formed, providing a more efficient molecular packing, and so that a substantially different methyl-methyl contact motif is created between adjacent molecular chains. The calculated enthalpies of the high-pressure and low-temperature structures shows that the high-pressure phase is the most energetically favorable. The relatively small 0.056 eV/molecule enthalpy difference between the two structures is reflected in the very low freezing pressure of approximately 0.2 GPa at room temperature compared to the freezing temperature of 16 °C at ambient pressure.

## II. STRUCTURE SOLUTION AND *AB INITIO* CALCULATIONS

For the ethanol and acetic-acid studies the experimental procedures were essentially the same. In both instances the liquid was loaded and pressurized in a Merrill-Bassett diamond-anvil cell<sup>15</sup> that had been equipped with 600- $\mu\text{m}$  culet diamonds and a steel gasket. After the nucleation of many crystallites the temperature was cycled close to the melting curve, in order to reduce the number of crystallites, in a manner similar to Ref. 16. Finally, a single crystal was obtained [at 3.0(1) GPa for ethanol and at 0.2 GPa for acetic acid] that entirely filled the 200- $\mu\text{m}$  gasket hole.

The setting angles of 25 strong reflections were determined for both samples on an Enraf-Nonius CAD4 diffractometer (equipped with a Mo x-ray tube) and a least-squares fit gave the monoclinic unit-cell parameters of ethanol to be  $a = 7.602(3)$  Å,  $b = 4.767(3)$  Å,  $c = 7.265(3)$  Å, and  $\beta = 114.80(3)^\circ$  with a volume  $V = 239.0(4)$  Å<sup>3</sup>; and the monoclinic unit-cell parameters of acetic acid to be  $a = 4.0365(12)$  Å,  $b = 13.2234(13)$  Å,  $c = 5.6979(8)$  Å and  $\beta = 91.912(17)^\circ$  with a volume  $V = 303.96(13)$  Å<sup>3</sup>. Comparing the unit-cell volume of the high-pressure phases with those of the low-temperature phases,<sup>7,17</sup> we expect there to be four molecules in the unit cell for both ethanol and acetic acid.

Intensity data were collected for both samples with the

TABLE I. Fractional coordinates of the 3.0 GPa ethanol structure obtained from the *ab initio* calculations (second set of coordinates) and, for comparison, the coordinates of the C/O atoms obtained from the single-crystal x-ray results (first set). The ESD's from single-crystal refinements are shown in parenthesis. The numerical accuracy of the *ab initio* calculations is within the number of decimal places quoted. C<sub>1</sub>, H<sub>1</sub>, H<sub>2</sub>, and H<sub>3</sub> form the CH<sub>3</sub> group, C<sub>2</sub>, H<sub>4</sub>, and H<sub>5</sub> form the CH<sub>2</sub> group; and O<sub>1</sub> and H<sub>6</sub> form the OH group of an ethanol molecule.

Element	Experimental			Theoretical		
	<i>x</i>	<i>y</i>	<i>z</i>	<i>x</i>	<i>y</i>	<i>z</i>
O <sub>1</sub>	0.9323(6)	0.3022(13)	0.1618(6)	0.9429	0.2763	0.1750
C <sub>1</sub>	0.6985(9)	-0.0219(21)	-0.0554(9)	0.6950	0.0142	-0.0704
C <sub>2</sub>	0.7525(11)	0.2754(25)	-0.0025(10)	0.7691	0.3003	0.0076
H <sub>1</sub>				0.6629	-0.1058	0.0385
H <sub>2</sub>				0.5575	0.0344	-0.2112
H <sub>3</sub>				0.7995	-0.1006	-0.1067
H <sub>4</sub>				0.7877	0.4222	-0.1103
H <sub>5</sub>				0.6631	0.4124	0.0456
H <sub>6</sub>				0.9872	0.4627	0.2312

$\omega$ -scan method at the position of least attenuation of the pressure cell, according to the fixed- $\phi$  technique.<sup>18</sup> All accessible reflections were measured in the shell  $h, \pm k, \pm l$  for  $0 \text{ \AA}^{-1} < \sin \theta/\lambda < 0.71 \text{ \AA}^{-1}$ . The intensities were corrected for absorption, averaged over Friedel pairs, and then used for structure solution by direct methods.<sup>19</sup> The systematic absences of the reflections indicated that the structure of ethanol has  $P2_1/c$  symmetry and a trial solution in this symmetry was found to be acceptable. The  $P2_1/c$  model was refined using the RFINE90 suite of programs<sup>20</sup> and the final structural parameters to the fit ( $R_w=0.17$ ,  $GoF=1.48$  for 487 reflections) are presented in Table I. For acetic acid, the systematic absences of the reflections indicated that the structure had the  $P2_1/n$  space group and trial solutions were attempted in this symmetry. The final model was refined using the RFINE90 suite of programs,<sup>20</sup> after averaging the reflections over symmetry equivalents, and the final structural parameters to the fit ( $R_w=0.14$ ,  $GoF=1.30$  for 605 reflections) are presented in Table II.

The x-ray-diffraction results give a reliable model for the high-pressure structures. However, from the available data, we are unable to determine the position of the hydrogens. Therefore a series of *ab initio* calculations have also been performed to calculate the full structure including hydrogen positions. The experimentally determined unit-cell param-

eters and the C and O positions are used as a starting point for the calculations and approximate positions for the hydrogen atoms are assumed. We then perform calculations based on the density-functional formalism within the generalized gradient approximation for the exchange and correlation potential.<sup>26</sup> The valence electron wave functions are expanded in a plane-wave basis to an energy cutoff of 700 eV that converges the total energy of the system to better than 1 meV/molecule.  $Q_c$ -tuned pseudopotentials of Lin *et al.*<sup>21</sup> in Kleinman-Bylander form<sup>22</sup> are used to describe the ion electron interactions. Integrations over the Brillouin zone are performed using a Monkhorst-Pack set of  $k$  points. We find that four  $k$ -points for ethanol and six  $k$ -points for acetic acid again converge the total energy of the system to better than 1 meV/molecule. The total energy of the system is minimized by varying the plane-wave coefficients using a preconditioned conjugate gradients scheme.<sup>23</sup> From a given relaxed electronic configuration the *ab initio* forces on each atom and the stresses on the unit cell are calculated and relaxed under a conjugate gradients algorithm. We consider the calculation converged when the components of all forces are below 0.01 eV/Å. We also simultaneously perform relaxation of the unit-cell parameters using *ab initio* stresses and an external pressure set to the experimental value. For this, a Pulay correction is required to maintain a constant energy cutoff for

TABLE II. Atomic coordinates of the high-pressure structure of acetic acid found by both x-ray diffraction and *ab initio* calculations at 0.2 GPa. The lattice parameters are given in the main text.

Element	Experimental			Theoretical		
	<i>x</i>	<i>y</i>	<i>z</i>	<i>x</i>	<i>y</i>	<i>z</i>
C <sub>1</sub>	0.3691(25)	0.4131(3)	0.2247(14)	0.3589	0.4128	0.2249
C <sub>2</sub>	0.2670(22)	0.3352(3)	0.3919(13)	0.2648	0.3329	0.3980
O <sub>1</sub>	0.3498(15)	0.2476(2)	0.3881(10)	0.3482	0.2505	0.3778
O <sub>2</sub>	0.0982(15)	0.3704(2)	0.5684(8)	0.0907	0.3621	0.5635
H <sub>1</sub>				0.7231	0.6091	0.9457
H <sub>2</sub>				0.7390	0.5135	0.7268
H <sub>3</sub>				0.3770	0.5833	0.7930
H <sub>4</sub>				0.9820	0.6923	0.3239

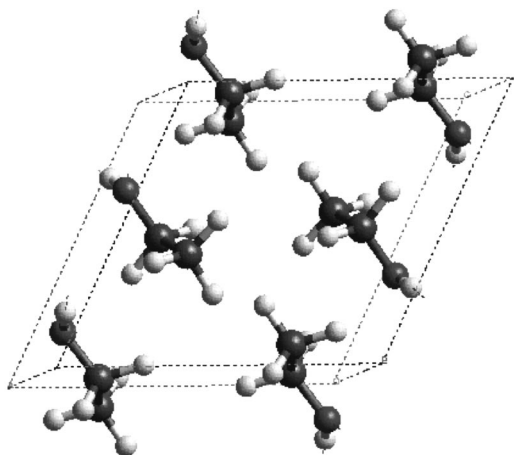


FIG. 1. The structure of crystalline ethanol at 3.0 GPa is shown. A clearer illustration of the hydrogen-bonded chains is given in Fig. 2.

the basis set expansion of the wave function due to the changing unit-cell parameters. From this we are able to determine the fully relaxed structural parameters including unit-cell parameters and the positions of the hydrogen atoms of the high-pressure ethanol and acetic-acid structures. As an additional test of the experimental results, we also performed the *ab initio* calculations without constraining the structures to any space group to look for any deviations from the allowed structural parameters of the  $P2_1/c$  and  $P2_1/n$  space groups for ethanol and acetic acid, respectively. It was found that the symmetry of the structure was preserved to within the accuracy of the calculations.

### III. RESULTS AND DISCUSSION

#### A. Ethanol

We performed *ab initio* calculations with full structural relaxation of all internal and unit-cell parameters at 3.0 GPa to give a direct comparison to experiment. The unit-cell parameters were found to be  $a=7.606$  Å,  $b=4.754$  Å,  $c=7.278$  Å, and  $\beta=116.92$  giving a unit-cell volume of  $234.68$  Å<sup>3</sup>. This is in excellent agreement with the experimental unit-cell parameters presented above.

The full structure of ethanol at 3.0 GPa, including the positions of the hydrogen atoms, is shown in Fig. 1. It can be seen that the molecules form linear hydrogen-bonded chains, parallel to the  $b$  axis, consistent with the formation of one hydrogen bond per molecule.

To make a quantitative comparison between the high-pressure and low-temperature structures of ethanol, we have also performed an *ab initio* calculation of the low temperature structure. The unit cell is found to have lattice parameters (at 0 GPa) of  $a=5.527$  Å,  $b=7.000$  Å,  $c=8.227$  Å, and  $\beta=98.44$  giving a volume of  $314.83$  Å<sup>3</sup> per unit cell. As the volume per molecule of the low-temperature and high-pressure phases are experimentally  $74.6$  Å<sup>3</sup> and  $59.8$  Å<sup>3</sup>, respectively, (and  $78.7$  Å<sup>3</sup> and  $58.7$  Å<sup>3</sup>, theoretically), the high-pressure arrangement provides a more efficient molecular packing. Compared to the high-pressure structure, the alignment of the carboxyl groups is reversed in neighboring chains so that the centrosymmetry is preserved.

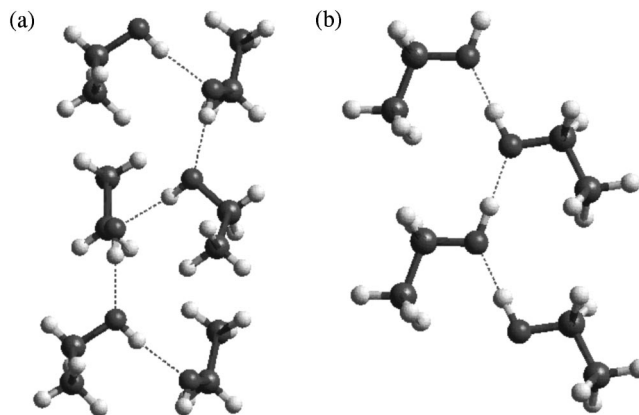


FIG. 2. The nature of the hydrogen-bonded chains in both (a) the low-temperature and (b) high-pressure structures of ethanol are illustrated here. In the low-temperature structure the H bonds are strained, while in the high-pressure structure the molecules are arranged so that the H-bond angles are close to an ideal  $180^\circ$ .

Within each chain in the high-pressure structure the molecules are coplanar and are aligned parallel to one another in an alternating 1-1-1 sequence. This arrangement is strikingly different from that of the low-temperature phase, shown in Fig. 2(a) where pairs of molecules are linked together in *trans* and *gauche* conformers with the carboxyl groups of each molecule directed away from the center of each pair. These molecular pairs alternate so that the molecules are arranged in a 2-2-2 sequence along the chain. In contrast, the molecules of the high-pressure phase, shown in Fig. 2(b), have only the *trans* conformation and they are linked in each chain so that their carboxyl groups are aligned in the same direction along the  $b$  axis—so that an “interlocking” arrangement is formed.

In Table III we give a selection of bond lengths and angles of the 3.0 GPa structure of ethanol as found by both

TABLE III. Selected bond angles (in degrees) and bond lengths (in Å) of the high-pressure structure of ethanol from the experimental studies and the *ab initio* calculations. We have also performed an *ab initio* calculation using the same techniques on an isolated molecule to show the distortion of the molecule in the crystal as compared to the ideal gas-phase structure.

Bond	Experimental	<i>Ab initio</i>	Isolated molecule
$O_1 \cdots H_6$		1.626	
$O_1-H_6$		0.970	0.958
$C_2-O_1$	1.393(8)	1.336	1.403
$C_1-C_2$	1.481(15)	1.484	1.498
$C_2-H_4$		1.097	1.101
$C_2-H_5$		1.101	1.101
$C_1-H_1$		1.091	1.092
$C_1-H_2$		1.087	1.092
$C_1-H_3$		1.091	1.092
Angle			
$O_1-H_6 \cdots O_1$		178.8	
$H_6-O_1-C_2$		132.5	110.0
$O_1-C_2-C_1$	112.1(8)	108.5	108.3

the experimental and theoretical methods. To illustrate the distortion of the molecules within the crystal we have also performed *ab initio* calculations to obtain the structure of the gas-phase ethanol molecule. A comparison of the structures is also presented in Table III. It can be seen that the major distortion of the ethanol molecule away from its gas-phase structure occurs in the length of the CO bond where it increases by  $\sim 10\%$  and also a distortion in the HOC angle. This angle opens by a relatively large amount, but the cost of this is offset by reducing the length of the hydrogen bond and also in a reduction of the H-bond strain angle.

As the space-group symmetry of the low-temperature phase requires two molecules in the *Pc* asymmetric unit (the *trans* and the *gauche* forms) its molecular chains are more irregular than those of the high-pressure phase where only one molecule is required in the *P2<sub>1</sub>/c* asymmetric unit (the *trans* form). For the low-temperature structure the C-C and C-O bond lengths are 1.512(3) Å and 1.499(3) Å for the *trans* conformation and 1.422(2) Å and 1.431(2) Å for the *gauche* conformations,<sup>7</sup> while the C-C-O bond angles are 108.8° and 112.0°, respectively. As expected, the corresponding bond lengths are somewhat smaller in the high-pressure phase where the C-C bond length is 1.484 Å while the length of the C-O bond is 1.336 Å. The C-C-O bond angle is 108.5°, which is close to that of the *trans* molecule in the low-temperature structure. The C-H distances show little variation in the high-pressure structure, differing at most by 0.006 Å from their average value of 1.093 Å. This compares favorably with the low-temperature phase where a mean C-H bond length of 0.98 Å is found.<sup>7</sup> The intermolecular hydrogen bonds for the low-temperature phase are also irregular as expected: the O-H distances vary between 0.79(4) Å and 0.85(3) Å and the H $\cdots$ O distances between 1.93(4) Å and 1.88(3) Å. Similarly, the O-H $\cdots$ O bond angles range from 176° to 172°. This contrasts with the high-pressure phase where the O-H and H $\cdots$ O distances and the O-H $\cdots$ O bond angles are equal by symmetry and have values of 0.970 Å, 1.626 Å, and 178.8°, respectively.

### B. Acetic acid

Our *ab initio* relaxed lattice parameters at 0.2 GPa are  $a=4.117$  Å,  $b=13.232$  Å,  $c=5.740$  Å, and  $\beta=92.42^\circ$ , which are in excellent agreement with experimental results. The full *ab initio* structure is shown in Fig. 3 and the structural parameters are given in Table II along with the experimental C and O coordinates. We have also carried out calculations of the low-temperature structure of acetic acid to compare with the high-pressure structure. A comparison of the high-pressure structure with the low-temperature structure reveals that the *trans* molecules in both structures are very similar and they link together in hydrogen-bonded molecular chains that are essentially identical. For the carboxyl groups in the high-pressure structure the C-O and C=O bond lengths are 1.274 Å and 1.150 Å for the high-pressure phase, and 1.321 Å and 1.206 Å for the low-temperature phase, while the O-C=O bond angles are 120.7° and 121.9°, respectively. The C-C distances are also very similar and are 1.512 Å and 1.501 Å for the high-pressure and low-temperature structures, respectively. The hydrogen-bond distances and angles, O-H, O $\cdots$ H, and O-H $\cdots$ O are 1.021 Å,

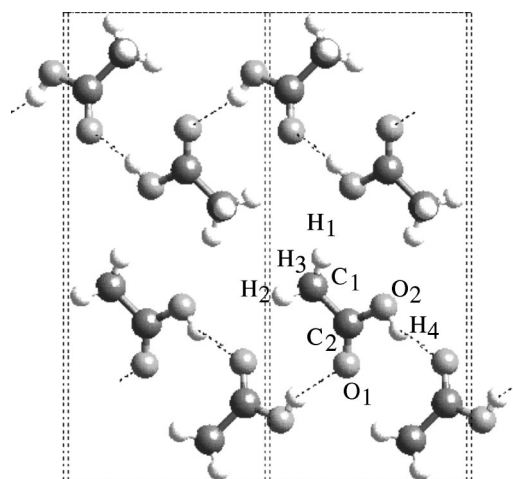


FIG. 3. Schematic illustration of the high-pressure structure of acetic acid at 0.2 GPa and room temperature. The dashed lines indicate hydrogen bonds.

1.910 Å, and 166.6° for the high-pressure structure and 1.011 Å, 1.642 Å, and 164.8° for the low-temperature structure — revealing, again, no substantial differences. For the high-pressure phase, we summarize the bond lengths in Table IV.

In the high-pressure structure, however, neighboring chains are oriented in an opposite sense from those in the low-temperature structure and, as can be seen in Fig. 4, this leads to the formation of puckered molecular layers accompanied by a more efficient molecular packing: in the low-temperature structure, at 278 K,<sup>24</sup> each molecule occupies a volume of 78.51 Å<sup>3</sup> while at high-pressure the molecular volume is 75.99 Å<sup>3</sup>. More significantly, though, this reorientation of the molecular hydrogen-bonded chains leads to a substantially different methyl-methyl contact motif between adjacent molecular chains. As is illustrated in Fig. 5, the low-temperature structure is characterized by methyl-methyl interactions, on the order of 4.0 Å, where the axes of the molecules (defined by the C-C bonds) are approximately perpendicular to one another and are directed towards the methyl carbon of the adjacent interacting molecule. These methyl-methyl contacts zig-zag in a direction parallel to the c

TABLE IV. As Table III, but for the high-pressure acetic-acid structure.

Bond	Experimental	<i>Ab initio</i>	Isolated molecule
C <sub>1</sub> –C <sub>2</sub>	1.472(7)	1.512	1.485
C <sub>2</sub> –O <sub>1</sub>	1.205(6)	1.150	1.196
C <sub>2</sub> –O <sub>2</sub>	1.318(5)	1.274	1.349
O <sub>2</sub> –H <sub>4</sub>		1.021	0.974
C <sub>1</sub> –H <sub>1</sub>		1.063	1.093
C <sub>1</sub> –H <sub>2</sub>		1.095	1.088
C <sub>1</sub> –H <sub>3</sub>		1.098	1.088
H <sub>4</sub> $\cdots$ O <sub>1</sub>		1.091	
Angle			
C <sub>1</sub> –C <sub>2</sub> –O <sub>1</sub>	125.2(4)	120.7	125.3
C <sub>1</sub> –C <sub>2</sub> –O <sub>2</sub>	114.2(3)	116.5	112.3

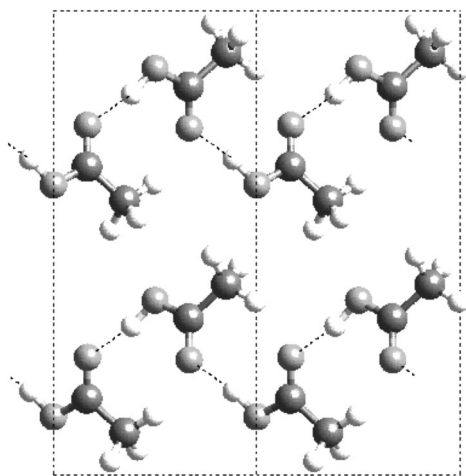


FIG. 4. A “ball and stick” illustration of the low-temperature structure of acetic acid.

axis linking molecules in adjacent hydrogen-bonded chains. In contrast, the methyl-methyl contact motif of the high-pressure phase involves only individual pairs of molecules, on neighboring chains, where their molecular axis are almost perfectly coincident and where their carboxyl groups are essentially coplanar (shown in Fig. 6), as well as marginally improving the packing efficiency.

#### IV. CONCLUSIONS

Although the molecules of the high-pressure phase of ethanol have a similar geometry to those of the *trans* conformations of the low-temperature structure, the connectivity within the hydrogen-bonded chains is markedly different. The O-H...O bond angles in the high-pressure structure are

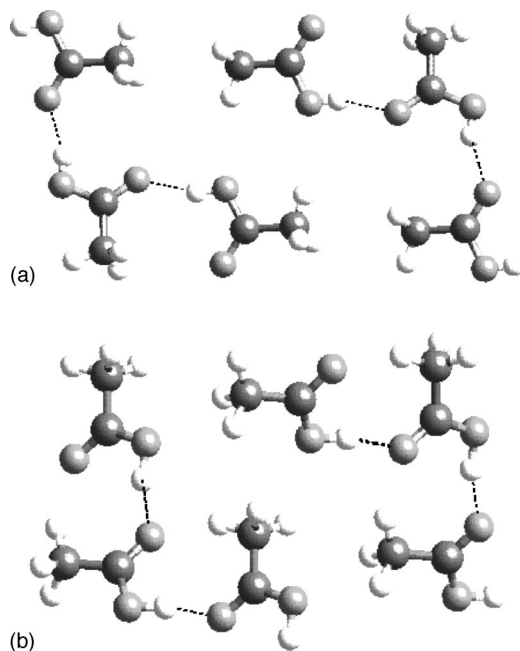


FIG. 5. A comparison between the methyl-methyl interactions of the (a) high-pressure and (b) low-temperature structures of acetic acid showing the “parallel” and “perpendicular” arrangements of the methyl groups.

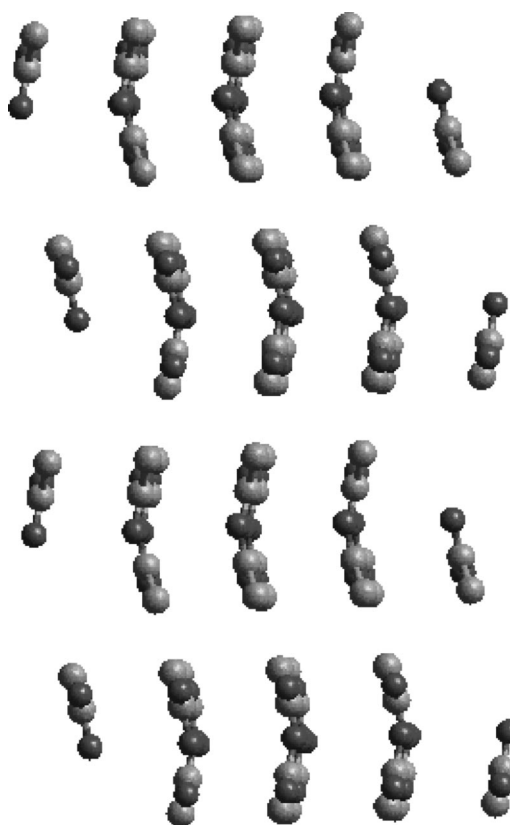


FIG. 6. A diagram of the high-pressure structure of acetic acid is shown with the hydrogen atoms removed for clarity. The planar configuration of the acetic-acid molecules can be seen.

equal by symmetry and are close to the ideal value of  $180^\circ$  while, by contrast, those of the low-temperature structure have differing values that are significantly distorted from colinearity. In the high-pressure phase of methanol<sup>2</sup> a similar effect was observed where the O-H...O bond angles range from  $150.9^\circ$  to  $178.2^\circ$  and it was concluded that the hydrogen-bonded chains of methanol molecules were highly strained relative to both of the low-temperature structures. For ethanol, the reverse appears to be the case and the chains of molecules in high-pressure phase are under less strain than those in the low-temperature structure. The strain in the high-pressure methanol phase is related to the 2-1-2-1 arrangement of the molecules, which is alleviated in the low-temperature forms by the molecules adopting the alternating 1-1-1 sequence.<sup>2</sup> This is also the case in ethanol where the structure exhibiting the least strain also adopts the 1-1-1 arrangement — although for ethanol it is the high-pressure phase. The strained structures (the low-temperature 2-2-2 phase of ethanol and the high-pressure 2-1-2-1 phase of methanol) both have molecules arranged in parallel within the chains. The proximity of the  $\text{CH}_3\text{CH}_2$  groups in ethanol and the  $\text{CH}_3$  groups in methanol lead to strong intermolecular repulsions for the parallel molecules, which appears then to lead to this strain.

In our recent study of formic acid it was concluded that, as for ethanol, the molecular chains in the high-pressure structure were under less strain than those in the low-temperature structure<sup>3</sup> and it was proposed that the formation of both *cis* and *trans* conformers in the high-pressure phase is the major factor in the mediation of this strain. The high-

pressure and low-temperature structures of acetic acid, however, have only the *trans* molecular conformation and, as mentioned above, they exhibit very similar O-H...O bond angles and subsequently virtually identical strains. The strain is, however, significantly greater than the strain in both the high-pressure and low-temperature structures of formic acid.<sup>3</sup> This indicates that although the reorientation of the molecular chains in the high-pressure acetic-acid structure allows a much simpler methyl-methyl interaction motif, and a more efficient molecular packing, it does not lead to a reduction in the strain within the molecular chains — which must accommodate the relatively large methyl groups. As already stated, all the other larger monocarboxylic acids (such as the next members the series, acrylic acid and propionic acid) form low-temperature crystal structures with isolated dimer pairs. This suggests that the “tail” on the carboxyl group cannot extend to more than one carbon (or a single methyl group) before the increased intermolecular repulsions leads to excessive strain in the hydrogen bonds for chain formation, and dimers result.

Finally, it is instructive to note that the larger linear alcohols  $H(CH_2)_nOH$  with  $n > 2$ , such as propanol and butanol do not crystallize either on cooling or compression but instead they invariably form glasses. This is somewhat differ-

ent than the behavior of the monocarboxylic acids where crystallization normally occurs even for extremely large molecules [for example valeric acid,  $CH_3CH_2CH_2CH_2COOH$  (Ref. 25)]. This suggests that hydrogen bonding in the monoalcohols is not strong enough, even at high pressure, to stabilize the increasingly flexible molecules into uniform conformations within a crystalline structure. In addition, although it is also possible to predict a possible route to dimer formation in formic acid where “near dimers” are formed at high pressure,<sup>3</sup> a similar mechanism is not so apparent in acetic acid. However, given that the strain on the hydrogen bonds is likely to increase with pressure, with the strengthening intermolecular repulsion from the methyl groups, it is anticipated that this may lead to the increased likelihood of dimer formation.

#### ACKNOWLEDGMENTS

We thank H. Vass for his help in maintaining and preparing the x-ray-diffraction facilities. We wish to thank G.J. Ackland for useful discussions. This work was supported by a grant from the Engineering and Physical Sciences Research Council.

- 
- <sup>1</sup> *Simple Molecular Systems at High Pressure*, edited by A. Polian, P. Loubeyre, and N. Boccarda (Plenum, New York, 1988).
- <sup>2</sup> D.R. Allan, S.J. Clark, M.J.P. Brugmans, G.J. Ackland, and W.L. Vos, *Phys. Rev. B* **58**, 11 809 (1998).
- <sup>3</sup> D.R. Allan and S.J. Clark, *Phys. Rev. Lett.* **82**, 3464 (1999).
- <sup>4</sup> C.P. Brock and L.L. Duncan, *Chem. Mater.* **6**, 1307 (1994).
- <sup>5</sup> K.J. Tauer and W.N. Lipscomb, *J. Chem. Phys.* **5**, 606 (1952); B.H. Torrie, S.-X. Weng, and B.M. Powell, *Mol. Phys.* **67**, 575 (1989).
- <sup>6</sup> A.H. Narten and A. Habenschuss, *J. Chem. Phys.* **80**, 3387 (1989).
- <sup>7</sup> P.G. Jonsson, *Acta Crystallogr., Sect. B: Struct. Crystallogr. Cryst. Chem.* **B32**, 232 (1976).
- <sup>8</sup> M.J.P. Brugmans and W.L. Vos, *J. Chem. Phys.* **103**, 2661 (1995).
- <sup>9</sup> M.J.P. Brugmans, Ph.D. thesis, University of Amsterdam, 1995.
- <sup>10</sup> D.C. Steytler, J.C. Dore, and D.C. Montague, *J. Non-Cryst. Solids* **74**, 303 (1985).
- <sup>11</sup> J.F. Mammone, S.K. Sharma, and M. Nicol, *J. Phys. Chem.* **84**, 3130 (1980).
- <sup>12</sup> H. Shimizu, Y. Nakamichi, and S. Sasaki, *J. Raman Spectrosc.* **21**, 703 (1990).
- <sup>13</sup> H. Shimizu, *Physica B & C* **139&140**, 479 (1986).
- <sup>14</sup> L.J. Root and B.J. Berne, *J. Chem. Phys.* **107**, 4350 (1997).
- <sup>15</sup> L. Merrill and W.A. Bassett, *Rev. Sci. Instrum.* **45**, 290 (1974).
- <sup>16</sup> W.L. Vos *et al.*, *Nature (London)* **358**, 46 (1992); *Phys. Rev. Lett.* **71**, 3150 (1993).
- <sup>17</sup> A. Albinati, K.D. Rouse, and M.W. Thomas, *Acta Crystallogr., Sect. B Crystallogr. Cryst. Chem.* **B34**, 2184 (1978).
- <sup>18</sup> L.W. Finger and H. King, *Am. Mineral.* **63**, 337 (1978).
- <sup>19</sup> A. Altomare, G. Cascarano, C. Giacovazzo, and D. Viterbo, *Acta Crystallogr., Sect. A: Found. Crystallogr.* **A47**, 744 (1991).
- <sup>20</sup> L.W. Finger and E. Prince, *A System of Fortran IV Computer Programs for Crystal Structure Computations*, Nat. Bur. Stad. (U.S.) No. 128 (U.S. GPO, Washington, DC, 1975).
- <sup>21</sup> J. S. Lin *et al.*, *Phys. Rev. B* **47**, 4174 (1993).
- <sup>22</sup> L. Kleinman and D. M. Bylander, *Phys. Rev. Lett.* **48**, 1425 (1982).
- <sup>23</sup> M.C. Payne, M.P. Teter, and J.D. Joannopolous, *Rev. Mod. Phys.* **64**, 1045 (1992).
- <sup>24</sup> I. Nahring, *Acta Chem. Scand.* **24**, 453 (1970).
- <sup>25</sup> R.F. Scheureman and R.L. Sass, *Acta Crystallogr.* **15**, 1244 (1962).
- <sup>26</sup> J.P. Perdew and Y. Wang, *Phys. Rev. B* **45**, 13 244 (1992).